KECK Geology Consortium
Learning Science Through Research
Published by the Keck Geology Consortium
Short Contributions
Keck Geology Consortium
Volume 33
May 2020
doi: 10.18277/AKRSG.2020.33.09

USING MICROLITES AND BUBBLES IN OBSIDIAN TO ASSESS FACTORS GOVERNING ERUPTION OF RHYOLITIC MAGMA

KURT KNESEL, Trinity University

INTRODUCTION

Deciphering the factors governing eruption of silicic magma is a fundamental problem in volcanology. A general model has emerged relating eruptive style to the interplay between ascent rate and the efficiency and extent of volatile loss during magma transport from subvolcanic chambers (e.g., Gonnermann and Manga, 2007). Fast ascent is believed to inhibit volatile loss, leading to bubble crowding, volatile overpressure and ultimately explosive fragmentation; in contrast, slow magma ascent favors gas escape and lava extrusion. Rise-rate estimates for magmas of andesitic and dacitic compositions are broadly consistent with this model (Rutherford and Gardner, 2000). However, comparable data for rhyolite eruptions has until recently been sparse (Castro and Gardner, 2008; Castro and Dingwell, 2009; Pallister et al., 2013; Tuffen et al., 2013; Myers et al., 2018), and the complex feedback between magma properties and processes during ascent that dictates degassing and eruptive behavior is only beginning to be understood (Cassidy et al., 2018).

This project aims to build a microtextural and chemical foundation from which to investigate conditions and processes governing eruption of rhyolitic magma. As a start, we focus on the effusive endmember, though we also consider explosively erupted products. Our textural analysis involves quantification of the size, shape, and orientation of microlites and bubbles in obsidian. In addition to providing insight into decompression-induced volatile loss and crystallization during magma ascent (e.g., Hammer and Rutherford, 2002; Toramaru, 2006; Cichy et al., 2011), microlite and bubble textures can be used to determine shear stresses and the type, magnitude, and rate of shear strain accumulated during magmatic flow (Manga, 1998; Castro et al., 2002; Rust et al., 2003; Rust and Cashman, 2007; Befus et al., 2014; 2015). We compliment these textural constraints by measuring the composition of phenocrysts and micro-phenocrysts to evaluate pre-eruptive conditions that influence magma ascent and emplacement.

The project kicked off with a visit to the spectacular Long Valley caldera in California to examine macro-scale flow structures on the well-preserved surfaces of young lava domes of the Inyo and Mono craters volcanic chains. Relocating to Trinity University in San Antonio, we then embarked on a 3D micro-textural and analytical study of flow-banded obsidian samples from heavily dissected and deeply exposed rhyolite lavas, pyroclastic deposits, and associated vent structures from the largest volcano in eastern Australia.

GEOLOGICAL BACKGROUND

Cenozoic volcanic rocks in Australia are almost entirely confined to the eastern edge of the continent (Fig. 1). This vast intraplate volcanic belt stretches some 3000 km from northern Queensland to Tasmania, and is mainly comprised of lava-field and central-volcano provinces (Wellman and McDougall, 1974). Although distinctions between the two province types are not always straightforward, the lava fields are commonly comprised of strongly undersaturated mafic lavas and show little to no age progression. In contrast, the central volcanoes consist mainly of mildly undersaturated to saturated mafic lavas with associated

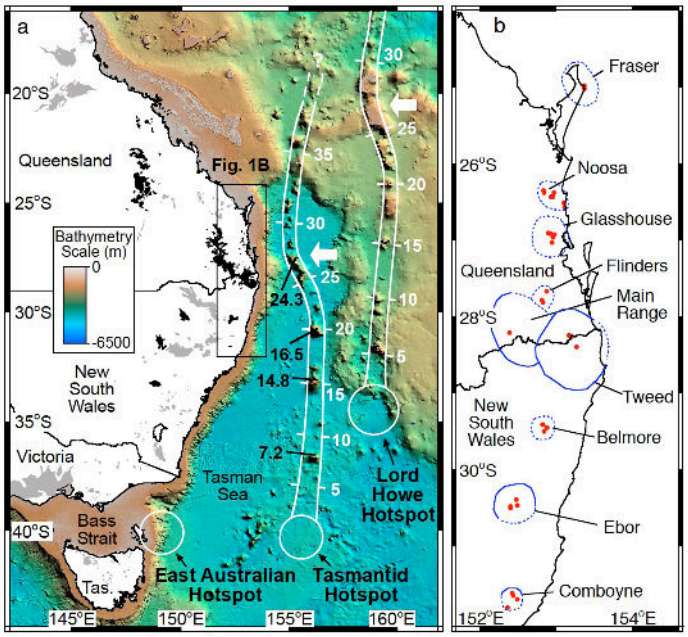

Figure 1. Distribution of Cenozoic volcanism on the Australian Plate, after Knesel et al. (2008). a, Central volcanoes are shaded black; mafic lava fields are grey; seamount tracks are outlined in white. White circles show predicted present-day hotspot locations. 40Ar/39Ar ages for Tasmantid seamounts from McDougall and Duncan (1988) are shown in black to the left of the chain; calculated ages are shown in white to the right of the two tracks at 5 Ma intervals. b, Locations of silicic rocks dated by 40Ar/39Ar geochronology (shown in red) from the central volcanoes (outlined in blue and dashed where approximate), including the Binna Burra Rhyolite, Tweed volcano).

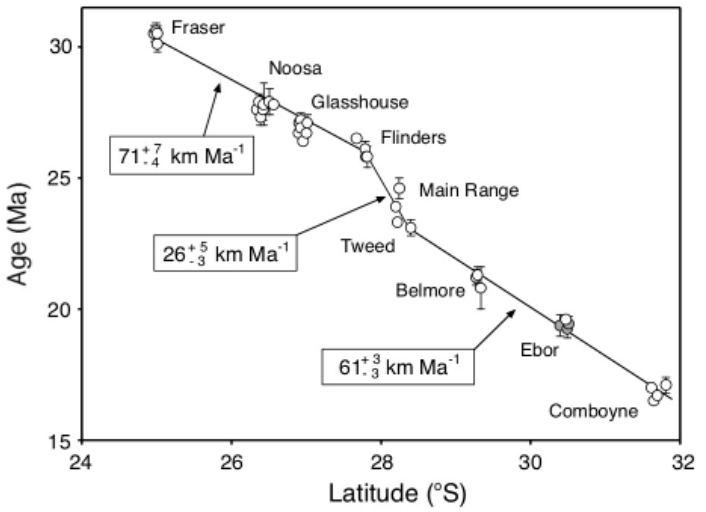

Figure 2. 40Ar/39Ar ages for silicic volcanic rocks from east Australian central volcanoes versus latitude, showing abrupt change in volcanic migration rate between 26-23 Ma, after Knesel et al. (2008). Ages for the Fraser, Noosa, Glasshouse, and Flinders areas are from Cohen et al. (2007); three (grey-filled symbols) of the four ages from Ebor volcano are from Ashley et al. (1995); all other ages for the Main Range, Tweed, Belmore, Ebor, and Comboyne volcanoes are from Knesel et al. (2008). Regressions of the 31-26 Ma, 26-23Ma, and 23-16 Ma time windows yield estimates for the northward component of Australian plate motion, relative to a fixed hotspot reference frame, shown with 1σ uncertainties..

felsic lava flows and intrusions that young southward. The age-progressive central volcanoes, along with the seamount tracks to the east (Fig. 1), are interpreted to track the northward movement of the Australian plate (Fig. 2) over several mantle hotspots over the past 35 Ma (Wellman and McDougall, 1974; McDougall and Duncan, 1988; Johnson, 1989; Sutherland, 2003; Vasconcelos et al., 2008).

The largest of the central volcanoes, the Tweed (or Mount Warning) volcano, straddles the border between the states of Queensland and New South Wales (Fig. 1). The Tweed volcano constitutes the eroded remnants of a former volcanic shield some 100 km in diameter (Fig. 3). River and stream incision has removed much of the northeastern flank and central region of the volcano, forming an erosional caldera some 30 km in diameter (Solomon, 1964). The volcano grew during a brief period of slow northward motion of the Australian Plate between ~26-23 Ma (Fig. 2) that has been linked to the onset of collision with the largest of the world's oceanic plateaus, the Ontong Java Plateau (Knesel et al., 2008). In addition to fueling the voluminous mafic volcanism, the longer time spent over the hotspot during the period of slow plate motion appears to have facilitated greater interaction between mafic magma and continental crust. The occurrence of silicic volcanism during this time window is anomalously high (Ewart et al., 1985), and includes rhyolite formations with isotopic signatures indicative of a predominantly crustal origin (Ewart, 1982).

An overview of the Tweed shield volcano (Fig. 3) is given in Ewart et al. (1987). The petrology and geochemistry of the volcanic succession comprising the northern flank of the volcano was examined by Ewart et al. (1977) and Ewart (1982). The stratigraphy of the southern flank of the volcano is presented in Duggan and Mason (1978) and a detailed evaluation of the petrogenesis was untaken by Duggan (1974). The generalized volcanic succession comprises an early mafic succession followed by rhyolitic lavas and tuffs that are in turn overlain by a younger mafic sequence. Two of the rhyolites – the Binna Burra and the Nimbin Rhyolites – are examined in this project.

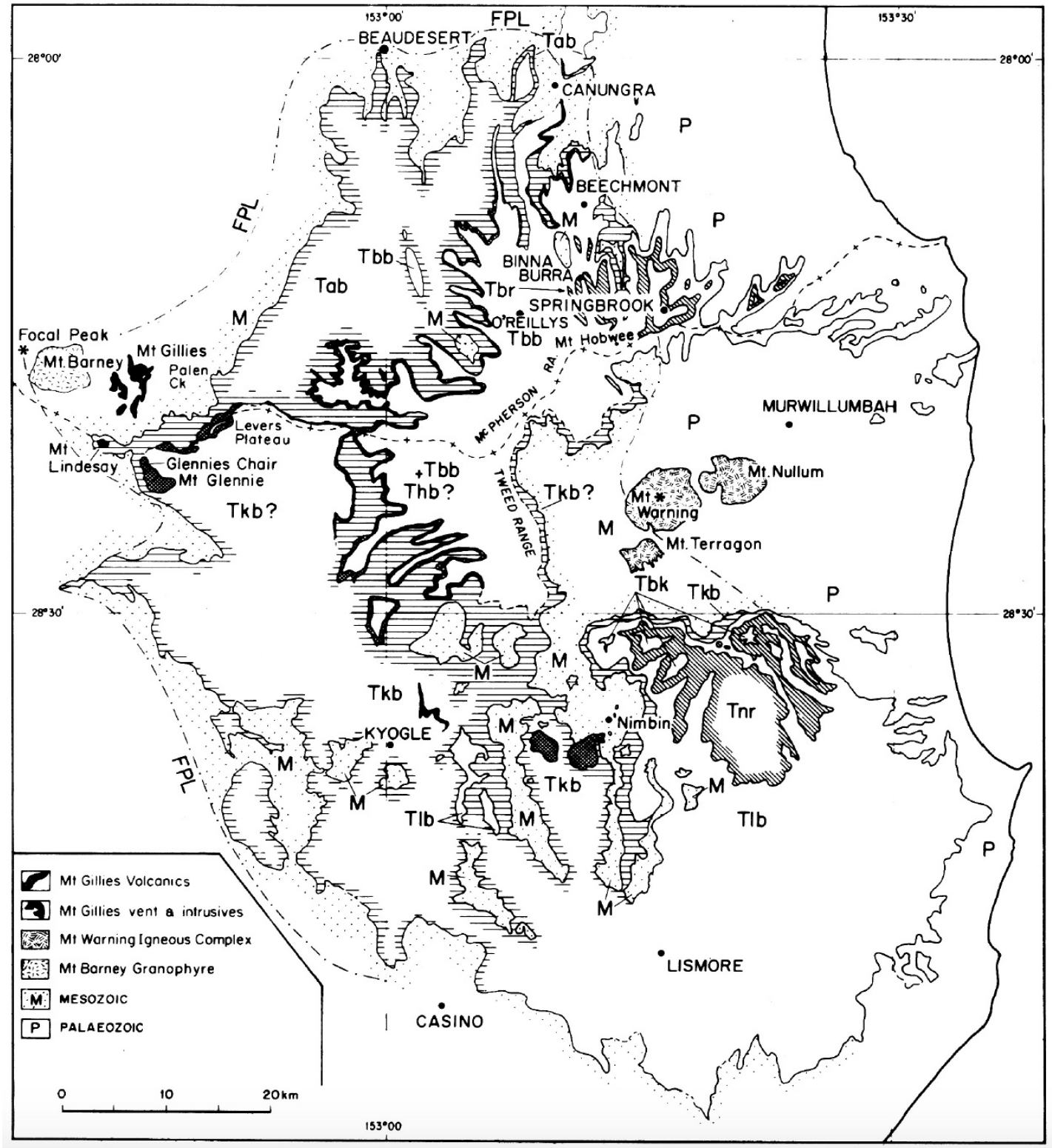

Figure 3. Geological map showing distribution of volcanic formations of the Tweed shield volcano, after Ewart et al. (1987). The volcanic succession consists of an early mafic sequence (Beechmont & Lismore Basalts) followed by rhyolitic lavas and tuffs (Binna Burra, Springbrook and Nimbin Rhyolites) that are overlain by a younger mafic sequence (Hobwee & Blue Knob Basalts). Basalts are shown in horizontally lined fields, while rhyolites are shown in diagonally lined fields. FPL: possible former limit of older basaltic lavas of the Focal Peak shield volcano (Albert & Kyogle Basalts). Thb: Hobwee Basalt, Tbk: Blue Knob Basalt, Tbr: Binna Burra and Springbrook Rhyolites, Tnr: Nimbin Rhyolite, Tbb: Beechmont Basalt, T1b: Lismore Basalt, Tab: Albert Basalt, Tkb: Kyogal Basalt, M: Mesozoic, P: Paleozoic.

The Nimbin Rhyolite is a complex of coalescing rhyolite lava domes and flows, along with minor pyroclastic deposits, erupted on the southern flank of the Tweed volcano (Fig. 3). The dome complex covers an area of roughly 400 km2 and reaches a maximum thickness of about 500 m. Individual lavas vary in thickness from 50 to 150 m and range from nearly aphyric to moderately porphyritic (10-30 vol. % crystals) flow-banded rhyolite, containing phenocrysts and micro-phenocrysts of quartz, sanidine, plagioclase, orthopyroxene, and minor clinopyroxene and ilmenite. Although extensive river and stream erosion have exposed the internal architecture of the domes and flows, dense vegetation limits access to most rock exposures. One voluminous lava flow defining the southern-most extent of the lava field, the Minyon Falls Rhyolite (Smith and Houston, 1995), affords excellent exposure of the basal obsidian, as well as the overlying crystalline core of the rhyolite, and was examined as part of all four student projects developed in this study.

The Binna Burra Rhyolite consists of at least five lava flows up to 100 m thick, with pyroclastic rocks at the base and near the top of the sequence, and includes a variety of plugs and dikes (Ewart et al., 1987). The pyroclastic rocks are predominantly fall deposits ranging from 20 to 120 m in thickness, but include at least one ash-flow tuff and boulder agglomerate. The rhyolite is biotite-bearing and thus is distinct from the rhyolite of the Nimbin dome complex. Sanidine from the Binna Burra Rhyolite yields an 40Ar/39Ar age of 23.9±0.2 Ma (Knesel et al., 2008). The conspicuous presence of volumetrically significant pyroclastic deposits, along with exposed vent structures, facilitated study of conditions and processes operating during shallow ascent of rhyolitic magma feeding both effusive and explosive activity.

STUDENT PROJECTS

Four students completed projects and submitted abstracts to the North Central GSA meeting in Duluth, MN (May, 2020). Summaries of their projects are presented below.

Chloe Campo (Trinity University) evaluated the influence of pre-eruptive magma temperature on the emplacement of rhyolite lava (Campo and Knesel, 2020). The chemical compositions of feldspars and pyroxenes were measured by scanning electron microscopy and were utilized, along with complimentary electron microprobe data, to calculate crystallization temperatures using the two-feldspar and two-pyroxene formulations described by Putirka (2008). Both thermometers indicate that micro-phenocrystic and groundmass minerals grew at pre-eruptive temperatures approximately 100ºC hotter than their phenocrystic counterparts and point to a late-stage thermal event driven by introduction of hot, mafic magma.

We then set out to establish whether the invading magma mixed with the rhyolite or simply transferred heat to it. Chemical analyses of colorless and brown-colored glassy flow bands within the rhyolite reveal that the bands are compositionally indistinguishable and, thus, are not likely the result of mixing of compositionally distinct magmas. This finding is consistent with analysis of microlite size and number densities indicating that flow banding in the rhyolite arose from degassing-related textural heterogeneities developed during shallow magma ascent (Seitzinger and Knesel, 2020; Seitzinger, this volume).

Chloe next explored the impact that pre-eruptive heating may have on the flow of lava. She discovered that the observed increase in temperature of about 100°C can produce a decrease in viscosity of roughly two orders of magnitude, and that this dramatic reduction may lead to a nearly 70% increase in the distance rhyolitic lava flows at the surface. Therefore, it appears that heating attendant with mafic recharge may not only trigger eruptions, it may also aid emplacement of highly degassed, aerially extensive silicic lava, without appealing to anomalously high eruption rates.

Brooke Dykstra (University of Illinois at Urbana-Champaign) investigated strain localization during emplacement of the Minyon Falls Rhyolite by examining the 3-dimensional orientation of acicular microlites in samples from the glassy base of the lava at near-vent and flow-front positions (Dykstra, Seitzinger and Knesel, 2020). The project benefitted from the dataset developed by Zenja Seitzinger in her study of microlite size and number densities

(summarized below); Brooke's measurements expanded the stratigraphic coverage of the near-vent site. Orientation distributions were characterized by the standard deviation (σ) of microlite trend (ϕ) and plunge (θ). Preliminary analysis reveals little to no systematic variation of microlite alignment with microlite size or with stratigraphic or lateral position within the basal shear zone. Samples with the greatest and least degree of alignment are within about 0.5 m of each other, and alignment varies by up to a factor of 4 among individual flow bands within a single thin section.

The orientations of microlites and flow bands around rotated phenocrysts indicate that strain in the basal obsidian was dominated by simple shear, although a component of pure shear is likely in some bands. Comparison of the measured microlite orientations to theoretically predicted distributions of slender rods in a Newtonian fluid in simple shear flow (Manga, 1998) yields strains ranging from 2 up to 10 in both near-vent and flow-front positions. Overall, the strain estimates are high compared to those estimated for obsidian samples collected near the upper surfaces of other rhyolite domes (Castro et al, 2002; Befus et al., 2014; 2015). This observation is consistent with structural analysis (Smith, 1996) and numerical results (Befus et al., 2015) indicating that most of the strain associated with emplacement of viscous rhyolite lava is accommodated within a basal zone of shear, while the main mass of lava is rafted above.

Juliana Flint (State University of New York, Plattsburg) assessed flow conditions of both explosively and effusively erupted rhyolite by measuring the shapes and orientations of deformed bubbles in obsidian samples from pyroclastic deposits and an exposed vent of the Binna Burra Rhyolite, as well as obsidian from the Minyon Falls Rhyolite (Flint and Knesel, 2020). The approach takes advantage of the fact that bubble deformation in a highly viscous, low Reynolds number fluid, such as rhyolitic magma, is governed by the competing shear stress that deform the bubble and the surface-tension stresses that minimize interfacial area (Rust and Manga, 2002; Rust et al., 2003). The ratio of these stresses is the capillary number, Ca. The relationships between Ca and the shape and orientation of bubbles were used to evaluate the type and magnitude of shear stress associated magma flow.

Bubble orientations in all samples are indicative of predominantly simple shear, although minor components of pure shear, bubble-bubble interactions, and bubble relaxation appear to have also influenced bubble shape and orientation in some instances. Bubble deformation is modest in the obsidian lava, yielding shear stresses of a few kPa. In contrast, bubble geometries in obsidian clasts from pyroclastic flow and fall units record the greatest deformation with shear stresses up to 90 kPa. Bubbles in samples from the dissected vent, thought to be associated with a boulder tuff (agglomerate), yield intermediate shear stresses of a few 10s of kPa. The observed increase in shear stress recorded in the lava, fountain-fed agglomerate, and pyroclastic flow and fall units is consistent with the general model in which eruption style is governed by ascent rate.

Zenja Seitzinger (State University of New York, Geneseo) investigated the timing and location of microlite and flow-band formation during effusive emplacement of rhyolite (Seitzinger and Knesel, 2020). The size, orientation, and number density of clinopyroxene microlites were measured in the basal obsidian from the Minyon Falls Rhyolite. The obsidian contains dark bands of microlite-poor brown glass and light bands of microlite-rich colorless glass. Textural measurements were made for up to nine individual bands within individual thin-section for samples collected from flow-front and near-vent locations.

Band thickness ranges from 45 microns to 6 mm and microlite number densities (MND) range from about 108 to 109 cm-3. Most of this range is present at the scale of a single thin section. Bands with higher MND have smaller average crystal sizes and steeper (negative) slopes on crystal sized distribution (CSD) plots, compared to bands with lower microlite number density. None of the microlite properties correlate with band thickness, degree of microlite preferred orientation, or position within the basal shear zone. This observation led Zenja to conclude that most microlites were apparently unable to nucleate or grow appreciably during flow on the surface and that the microlite-defined flow bands formed during magma ascent. Therefore, while microlite preferred

orientations within the basal shear zone register measurable re-orientation during emplacement (Dykstra, Seitzinger and Knesel, 2020), microlite number densities and size distributions reflect conduit processes. Given that number densities and size distributions of microlites vary on the scale of a thin-section, individual flow bands appear to record spatially complex variations in ascent rate, extent and/or depth of degassing, and residence time during transport in shallow volcanic conduits.

ACKNOWLEDGEMENTS

This material is based upon work supported by the Keck Geology Consortium and the National Science Foundation under Grant No. 1659322. We are grateful to Annie Barrett, Carol Blanchette and Chris Orr at the Valentine Eastern Sierra Reserves in Mammoth Lakes, CA, who provided us with an incredible experience at the Valentine Camp while in the field. This project benefitted greatly from the field work and exploratory research conducted by Anna Brown, Shari Cook, and Drew Luck at the University of Queensland.

REFERENCES

Ashley, P.M., Duncan, R.A., and Feebrey, C.A. (1995) Ebor Volcano and Crescent Complex, northeastern New South Wales: age and geological development. Australian Journal of Earth Science 42, 471-480.

Befus, K.S., Zinke, R.W., Jordan, J.S., Manga, M., and Gardner, J.E. (2014) Pre-eruptive storage conditions and eruption dynamics of a small rhyolite dome: Douglas Knob, Yellowstone volcanic field, USA. Bulletin of Volcanology 76, 1-12.

Befus, K.S., Manga, M., Gardner, J.E., and Williams, M. (2015) Ascent and emplacement dynamics of obsidian lavas inferred from microlite textures. Bulletin of Volcanology 77, 1-17.

Campo, C., and Knesel, K. (2020) Pre-eruptive temperatures and eruption dynamics of rhyolite lava, Nimbin Rhyolite dome complex, eastern Australia. Geological Society of America Abstracts with Programs 52, No. 5, doi: 10.1130/abs/2020NC-348134.

Cassidy, M., Manga, M., Cashman, K., and Bachman, O. (2018) Controls on explosive-effusive volcanic eruption styles: Nature Communications 9, 2839.

Castro, J., Manga, M., and Cashman, K. (2002) Dynamics of obsidian flows inferred from microstructures: insights from microlite preferred orientations. Earth and Planetary Science Letters 302, 38-50.

Castro, J.M., and Gardner, J.E. (2008) Did magma ascent rate control the explosive-effusive transition at the Inyo volcanic chain, California? Geology 36, 279-282.

Castro, J.M., and Dingwell, D.B. (2009) Rapid ascent of rhyolite magma at Chaiten volcano, Chile. Nature 461, 780-784.

Cichy, S.B., Botcharnikov, R.E., Holtz, F., and Behrens, H. (2011) Vesiculation and microlite crystallization induced by decompression: a case study of the 1991-1995 Mt Unzen eruption (Japan). Journal Petrology 52, 1469-1492.

Cohen, B.E., Vasconcelos, P.M., and Knesel, K.M. (2007) 40Ar/39Ar constraints on the timing of Oligocene intraplate volcanism in southeast Queensland. Australian Journal of Earth Science 54, 105-125.

Duggan, M.B. (1974) The mineralogy and petrology of the southern portion of the Tweed Shield Volcano, northeastern New South Wales, Unpubl. Ph.D. Thesis, Univ. of New England.

Duggan, M.B., and Mason, D.R. (1978) Stratigraphy of the Lamington Volcanics in far northeastern New South Wales, Journal of the Geological Society of Australia 25, 65-73.

Dykstra, B., Seitzinger, Z., and Knesel, K. (2020) Microlite orientations and strain localization within the basal shear zone of a large rhyolite lava dome, Minyon Falls, Australia. Geological Society of America. Abstracts with Programs 52, No. 5, doi: 10.1130/abs/2020NC-348339.

Ewart, A., Oversby, V.M., and Mateen, A. (1977) Petrology and Isotope Geochemistry of Tertiary Lavas from the Northern Flank of the Tweed Volcano, Southeastern Queensland, Journal of Petrology 18, 73-113.

Ewart, A. (1982) Petrogenesis of the Tertiary anorogenic volcanic series of southern Queensland, Australia, in light of trace element geochemistry and O, Sr, and Pb isotopes, Journal

of Petrology 23, 344-382.
Ewart, A., Chappell, B.W., and Le Maitre, R.W. (1985) Aspects of the mineralogy and chemistry of the intermediate-silicic Cainozoic volcanic rocks of eastern Australia. Part 1: introduction and geochemistry, Australian Journal of Earth Science 32, 359-382.
Ewart, A., Stevens, N.C., and Ross, J.A. (1987) The Tweed and Focal Peak shield volcanoes, southeastern Queensland and northeast New South Wales, Pap. Dep. Geol. Univ. Qd. 11 (4), 1-82.
Flint, J., and Knesel, K. (2020) Bubble shapes and orientations in obsidian lavas, pyroclasts, and vents of the Tweed shield volcano, eastern Australia. Geological Society of America Abstracts with Programs 52, No. 5, doi: 10.1130/abs/2020NC-348341.
Gonnermann, H.M., and Manga, M. (2007) The fluid mechanics inside a volcano. Annual Review of Fluid Mechanics 39, 321-356.
Hammer, J.E., and Rutherford, M.J. (2002) An experimental study of the kinetics of decompression-induced crystallization in silicic melt: Journal of Geophysical Research, v. 107, doi: 10.1029/2001JB000281.
Johnson, R.W. (1989) Intraplate volcanism in Eastern Australia and New Zealand, 408 p.
Knesel K.M., Cohen B.E., Vasconcelos P.M., and Thiede D.S. (2008) Rapid change in drift of the Australian plate records collision with Ontong Java Plateau, Nature 454, 754-757.
Manga, M. (1998) Orientation distribution of microlites in obsidian. Journal of Volcanology and Geothermal Research 86, 107-115.
McDougall, I., and Duncan, R.A. (1988) Age progressive volcanism in the Tasmantid Seamounts. Earth and Planetary Science Letters 89, 207-220.
Myers, M.L., Wallace, P.J., Wilson, C.J.N., Watkins, J.M., and Liu, Y. (2018) Ascent rates of rhyolitic magma at the onset of three caldera-forming eruptions. American Mineralogist 103, 952-965.
Pallister, J.S., Diefenbach, A.K., Burton, W.C., Munoz, J., Griswold, J.P., Lara, L.E., Lowenstern, J.B., and Valenzuela, C.E. (2013) The Chaiten rhyolite lava dome: Eruption sequence, lava dome volumes, rapid effusion rates and source of the rhyolite magma. Andean Geology 40, 277-294.
Putirka, Keith D. (2008) Thermometers and Barometers for Volcanic Systems: Reviews in Mineralogy and Geochemistry 69, 61-120.
Rust, A.C., and Manga, M. (2002) Bubble shapes and orientations in low Re simple shear flow. Journal of Colloid and Interface Science 249, 476-480.
Rust, A.C., Manga, M., and Cashman, K.V. (2003) Determining flow type, shear rate and shear stress in magmas from bubble shapes and orientations. Journal of Volcanology and Geothermal Research 122, 111-132,
Rust, A.C., and Cashman, K.V. (2007) Multiple origins of obsidian pyroclasts and implications for changes in the dynamics of the 1300 B.P. eruption of Newberry Volcano, USA. Bulletin of Volcanology 69, 825-845.
Rutherford, M.J., and Gardner, J.E. (2000) Rates of magma ascent. In Encyclopedia of Volcanoes (Ed. Sigurdsson, H.) 207-217.
Seitzinger, Z., and Knesel, K. (2020) Flow bands and microlite textures in obsidian, Minyon Falls Rhyolite, Australia. Geological Society of America Abstracts with Programs 52, No. 5, doi: 10.1130/abs/2020NC-348340.
Smith, J.V., and Houston, E.C. (1995) Structure of lava flows of the Nimbin Rhyolite, northeast New South Wales: Australian Journal of Earth Sciences 42, 69-74.
Smith, J.V. (1996) Ductile-brittle transition structures in the basal shear zone of a rhyolite lava flow, eastern Australia: Journal of Volcanology and Geothermal Research. 72, 217-223.
Solomon, P.J. (1964) The Mount Warning Shield Volcano: a general geological and geomorphological study of the dissected shield, Pap. Dep. Geol. Univ. Qd. 5 (10), 1-12.
Sutherland, F.L. (2003) 'Boomerang' migratory intraplate Cenozoic volcanism, eastern Australian rift margins and the Indian-Pacific mantle boundary, Geological Society of Australia Special Publication 22 & Geological Society of America Special Paper 372, 203-221.
Toramaru, A. (2006) BND (bubble number density) decompression rate meter for explosive eruptions. Journal of Volcanology and Geothermal Research 154, 303-316.
Tuffen, H., James, M.R., Castro, J.M., and Schipper,

C.I. (2013) Exceptional mobility of an advancing rhyolitic obsidian flow at Cordón Caulle volcano in Chile. Nature Communications 4, 2709.

Vasconcelos, P.M. Knesel, K.M., Cohen, B.C., and Heim, J.A. (2008) Geochronology of the Australian Cenozoic: a history of tectonic and igneous activity, weathering, erosion, and sedimentation, Australian Journal of Earth Science 55, 865-914.

Wellman, P., and McDougall, I. (1974) Cainozoic igneous activity in eastern Australia, Tectonophysics 23, 49-65.